

Characterization of Dynamic Mechanical Properties of Resistance Welding Machines

Relative displacement between electrodes was modeled and tested

BY P. WU, W. ZHANG, AND N. BAY

ABSTRACT. The dynamic mechanical properties of a resistance welding machine have significant influence on weld quality, which must be considered when simulating the welding process numerically. However, due to the complexity of the machine structure and the mutual coupling of components of the machine system, it is very difficult to measure or calculate the basic, independent machine parameters required in a mathematical model of the machine dynamics, and no test method has so far been presented in literature that can be applied directly in an industrial environment.

In this paper, a mathematical model characterizing the dynamic mechanical characteristics of resistance welding machines is suggested, and a test setup is designed determining the basic, independent machine parameters required in the model. The model is verified by performing a series of mechanical tests as well as real projection welds.

Introduction

The influence of mechanical machine properties on weld quality and electrode service life in spot and projection welding has been studied in recent years (Refs. 1–7). The large importance of the mechanical properties is realized and they may be of even greater importance than the electrical ones, especially when projection welding complex material combinations.

The mechanical machine properties are divided into static and dynamic ones. The static properties, which mainly affect the shape of the weld influenced by contact errors, are specified in ISO Standard 669 (Ref. 8). The dynamic properties are especially important in two phases of the welding cycle, i.e., in the squeeze phase

and in the welding phase. In the squeeze phase, the moving electrode approaches and touches the weld parts prior to welding causing an impulse and a sharp increase in the electrode force, and then follows an oscillation of the load until it reaches its set, static value. This load fluctuation results in high electrode wear but unrecognizable influence on weld quality since the electrode force is stabilized before current flow if the squeeze time is set appropriately. In the welding phase, a slight movement of the electrodes toward each other takes place due to plastic deformation of the workpieces as they soften or melt. Especially in projection welding, the electrode force drops in a brief, initial phase during welding due to collapse of the projection causing oscillations of the load or even loss of contact between electrode and workpiece, resulting in poor weld quality. To ensure good weld quality fast follow-up speed of the electrode is thus essential to compensate for the deformation or collapse of the weld parts. This is the most important feature as regards dynamic mechanical characteristics of resistance welding machines.

The dynamic response characteristics of resistance welding machines are normally considered to be governed by four factors (Refs. 2, 3, 5): the compression system of the load cylinder, the mass of the electrode head, the stiffness of the electrode systems, and the friction force. Some studies on the influence of the last three factors on welding process and weld quality have been reported in the literature (Refs. 1, 3–5) adjusting the factors on a specially designed simulating device or adding some additional components to the machine. Reference 2 analyzed the mechanical properties of a resistance spot

welding machine using a mathematical model. As a consequence, these results have provided a basis for modifying the design of the machines, improving the touching behavior and the follow-up ability, the latter by adding additional springs in the electrode head or increasing the stiffness of the lower electrode. But most of these investigations were limited to qualitative analysis presenting no modeling methods for simulation of the dynamic mechanical behavior in practice.

In this paper, a generic mathematical model of the mechanical system of resistance welding machines is proposed. A specially designed test setup (a mechanical breaking test) developed at the authors' department is applied and further developed to identify the machine parameters in the model (Refs. 9, 10). The method is validated by projection welding experiments.

Mathematical Model of Mechanical System

A lumped-mass damped vibratory unit is adopted as model of a C-frame resistance welding machine — Fig. 1. In the figure, m is the equivalent, lumped moving mass, including all moving masses (piston, sealing elements, electrode holders, etc.) and equivalent masses such as those from the flexible band conductors in the secondary circuit; b is the equivalent damping coefficient, which is mainly caused by friction on the moving components in the compression system; k is the equivalent spring constant, governed by the stiffness of piston rod, upper and lower electrode arms, machine frame including lower electrode arm support, and by the influence of compressed air in the cylinder and possible additional springs in the moving head; F is the total action force delivered by the moving electrode, including force delivered by the compression system in the cylinder and the force of gravity, i.e., $F = F_{cylinder} + mg$; and F_r is the reaction force from the workpiece on the moving electrode. After the squeeze stage, the electrode force is stabilized and reaches its static set value. At this moment, one may assume $F = F_r$.

KEYWORDS

Break Test
Dynamic Characteristics
Electrode Force
Mechanical Machine Properties
Projection Welding
Resistance Welding

P. WU is currently with the College of Machinery and Electrical Engineering, Inner Mongolia Agricultural University, Huhhot, P.R. China. The work was carried out at Technical University of Denmark. N. BAY is with the Department of Manufacturing Engineering and Management, Technical University of Denmark, Lyngby, Denmark. W. ZHANG is with SWANTEC Software and Engineering ApS, Hoersholm, Denmark.

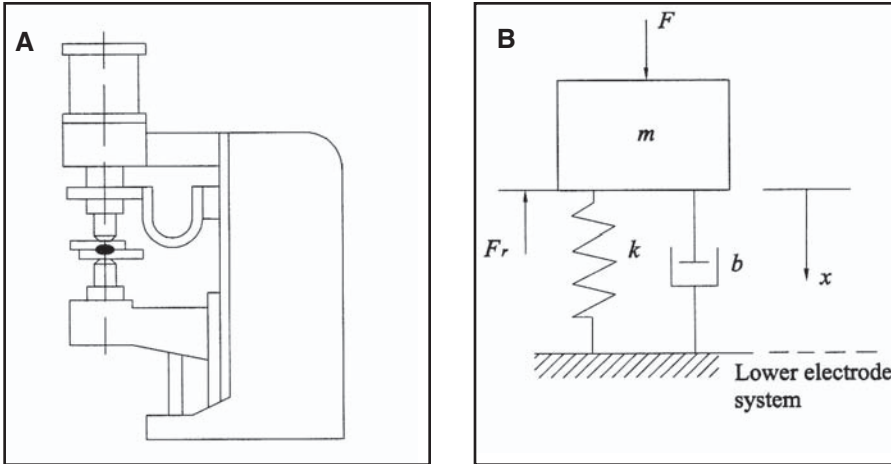


Fig. 1 — A — Schematic of C-frame resistance welding machine; B — mechanical model: m is the equivalent, lumped moving mass, b is the equivalent damping coefficient, k is the equivalent spring constant, F is the total action force delivered by the moving electrode, and F_r is the reaction force from the workpiece on the moving electrode.

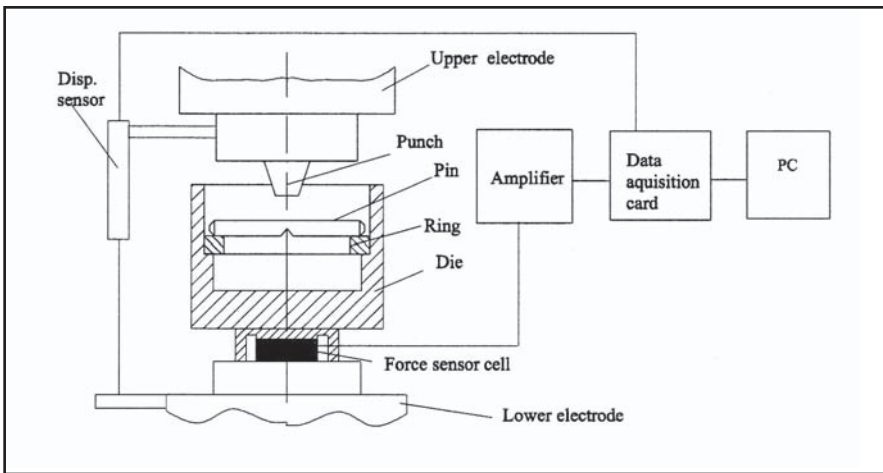


Fig. 2 — Experimental setup and measuring system.

When the current is applied, the reaction force decreases due to softening or melting of the weld parts resulting in plastic deformation of these and, in the case of projection welding, rapid collapse of the projection. The electrodes will move toward each other under the action of the compression force and elastic spring-back of the electrode arms. The relative movement between the two electrodes can be described by the following equation according to Newton's second law:

$$m \frac{d^2 x}{dt^2} + b \frac{dx}{dt} + kx = F - F_r \quad (1)$$

Principle of Determining the Machine Parameters

To solve the mathematical model above, the machine characteristic parameters (m , b , k) need to be determined. In

the special case of no reaction force from the workpiece, i.e., $F_r = 0$ corresponding to sudden collapse of the projection in projection welding or splash formation in spot welding, Equation 1 is reduced to

$$m \frac{d^2 x}{dt^2} + b \frac{dx}{dt} + kx = F \quad (2)$$

Loading experiments with sudden collapse of the load support were carried out in a special test setup designed earlier in the authors' department (Ref. 9). The test is schematically shown in Fig. 2. A hardened steel pin (DIN 6325, high-grade alloy steel 100Cr, 58~62 HRC) provided with a small notch in the middle was loaded to fracture by a punch mounted on the upper electrode, thus simulating the momentary removal of load support occurring in case of projection collapse in resistance weld-

ing. After pin fracture, the two electrodes were temporarily not in mechanical contact, resulting in the upper electrode moving down rapidly under the action of the force delivered by the load cylinder, and the lower electrode bouncing back due to spring-back of the prior loaded lower arm. The force F supplied to the upper electrode by the cylinder is assumed to be constant neglecting variation of cylinder pressure during pin fracture implying that the relative movement between the two electrodes is represented by Equation 2. Different levels of fracture load are applied by employing pins of different diameters. Since the upper electrode is moving freely, i.e., without support from the lower one after breaking of the pin, the test is named the "free breaking test."

During testing, the relative displacement x between the upper and lower electrodes is measured by a resistive-type displacement transducer — Fig. 2. The total action force F (equal to the breaking force of the pin) is measured by a piezoelectric load transducer mounted on top of the lower electrode. Measurements are recorded on a PC adopting a *LABVIEW* data-acquisition program. A sampling frequency of 30 kHz ensures enough data points for subsequent numerical differentiation determining the velocity \dot{x} and acceleration \ddot{x} . Equation 2 can be numerically presented in matrix form

$$\begin{bmatrix} \ddot{x}_1 \dot{x}_1 x_1 \\ \ddot{x}_2 \dot{x}_2 x_2 \\ \dots \dots \dots \\ \ddot{x}_n \dot{x}_n x_n \end{bmatrix} \begin{bmatrix} m \\ b \\ \dots \\ k \end{bmatrix} = \begin{bmatrix} F \\ F \\ \dots \\ F \end{bmatrix}, \quad [A] \cdot \begin{bmatrix} m \\ b \\ \dots \\ k \end{bmatrix} = [F] \quad (3)$$

In Equation 3, n corresponding values of x , \dot{x} , and \ddot{x} for a given breaking test with an action force F are inserted. The machine parameters m , b , k are determined by solving the n equations using the least-squares method in *MATLAB* (Ref. 11).

Free Breaking Tests

Free breaking tests were performed on a single-phase AC welding machine provided with an air-actuated loading system (TECNA 250kVA). The range of fracture forces investigated was 2 to 10 kN, which is the commonly used load range for the machine. Approximately 65 tests, with fracture loads rather evenly distributed within this range, were carried out using four different pin diameters (4, 5, 6, and 8 mm) and varying depths of the notch. As an example, Fig. 3 shows the load and displacement curves measured in the free breaking test when using a 5-mm-diameter pin. The pin fractures at a load $F = 4.72$ kN, after which the two elec-

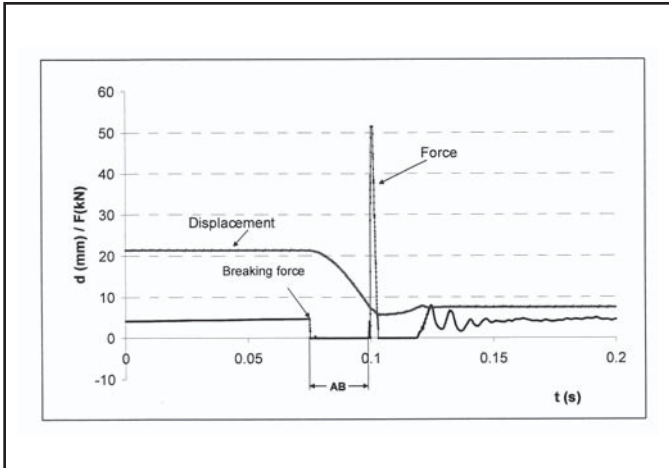


Fig. 3 — Measured load and displacement as functions of time for free breaking test on TECNA machine, fracture load 4.72 kN.

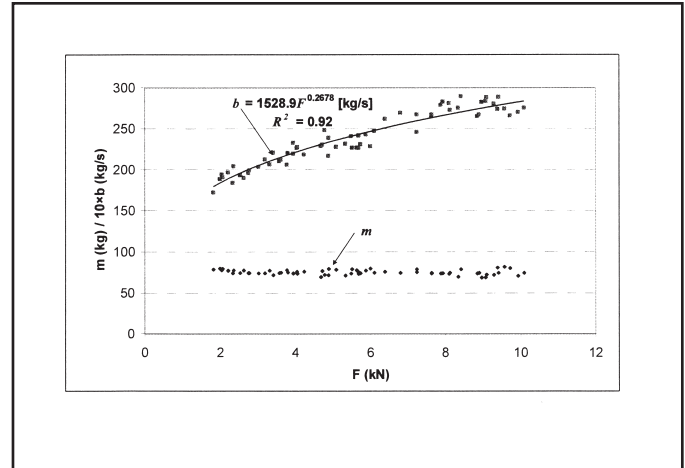


Fig. 4 — Equivalent mass and damping coefficient as a function of load.

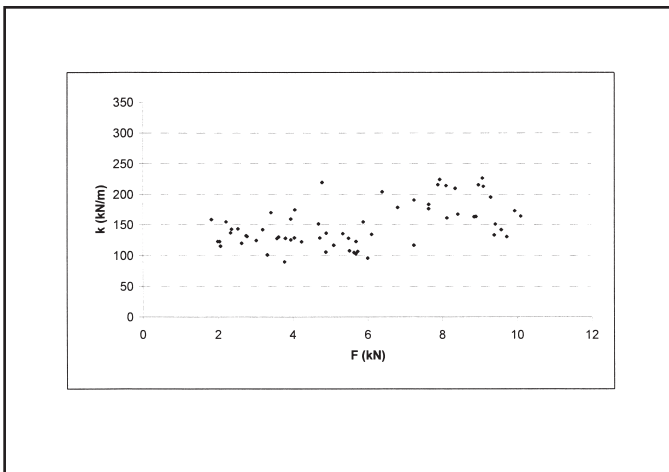


Fig. 5 — Equivalent spring constant as a function of load.

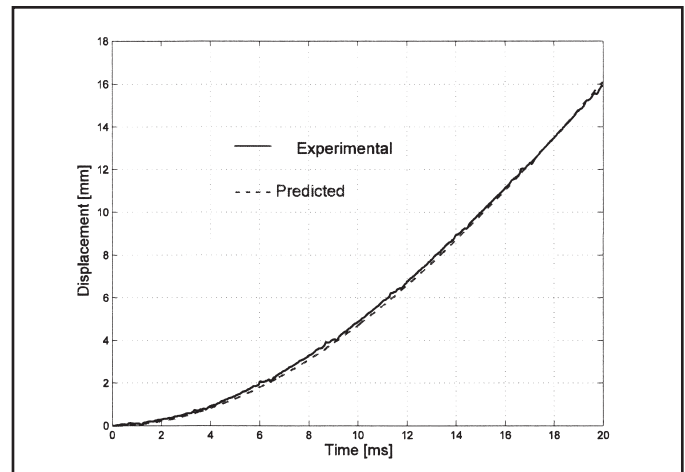


Fig. 6 — Experimental vs. predicted displacement at 8.1 kN.

trodes lose contact momentarily thus the reaction force drops to zero. The time range AB shown in Fig. 3 corresponds to the duration of lost contact of the electrodes after pin fracture. This is the time range of interest in the test. After the time AB, the two electrodes hit each other implying an abrupt increase in the load.

Figure 4 shows the determined values of equivalent mass m and damping coefficient b for the TECNA machine based on free breaking tests at different fracture loads. The equivalent mass is seen to be almost constant, i.e., independent of the load, and an average value of 75 kg is adopted, while the equivalent damping coefficient is noticed to increase with increasing load.

Figure 5 shows the equivalent spring constant vs. the load. Large scatter is observed, which might be due to the fact that the spring constant has much smaller influence on the electrode displacement than the other two parameters, since the term kx in Equation 1 is much smaller than

the two first terms. For this reason it is chosen to adopt the average value 150 kN/m, independent of the load. The assumption of constant mass and stiffness of the mechanical system is intuitively correct, since they are related to the structure of the mechanical machine components. On the other hand, the equivalent damping coefficient is a function of the load since it is mainly determined by friction on the moving components. The relation between damping coefficient and load is obtained by regression analysis of the F - b curve in Fig. 4. For the investigated machine, one gets

$$b = 1528.9 \times F^{0.2678} [\text{kg/s}]$$

where F is the load in kN. Figure 6 shows good fitting (residual error between experimental and predicted curve $R^2=1$) between experimentally measured and predicted displacement computed with the determined machine parameters at a load $F = 8.1$ kN ($m = 75$ kg, $b = 2677$ kg/s, $k = 150$ kN/m), while Fig. 7 showing the results at a load $F = 9.93$ kN ($m = 75$ kg, $b = 2905$

kg/s, $k = 150$ kN/m) represents the worst fitting among the tests, and yet still shows acceptable coincidence ($R^2 = 0.981$). In general, the agreement between measured and predicted displacement curves was fine, indicating that the proposed way of identifying the mechanical machine parameters is feasible.

Validation of the Model

Supported Breaking Tests

In order to check the validity of the mathematical model and the test method described above for the case, when a reaction force is present after pin fracture ($F_r \neq 0$), disk springs are added in the breaking test — Fig. 8. In this way, a reaction force F_r is introduced, which is varied by varying the stiffness level changing the number of springs as well as the way of stacking them (in parallel or series). Six different spring constants are applied: $k = 0.894, 1.795, 1.849, 2.654, 3.698,$ and 5.897

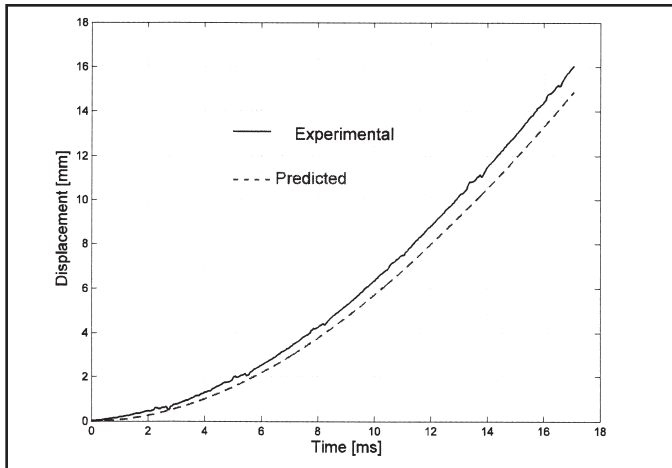


Fig. 7 — Experimental vs. predicted displacement at 9.93 kN.

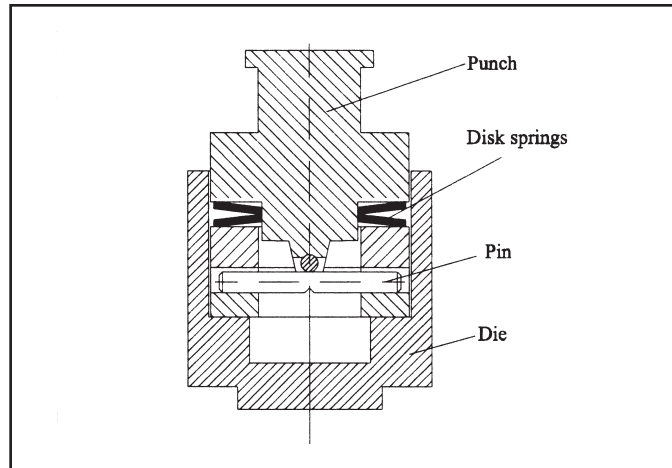


Fig. 8 — Supported breaking test setup with disk springs providing reaction force.

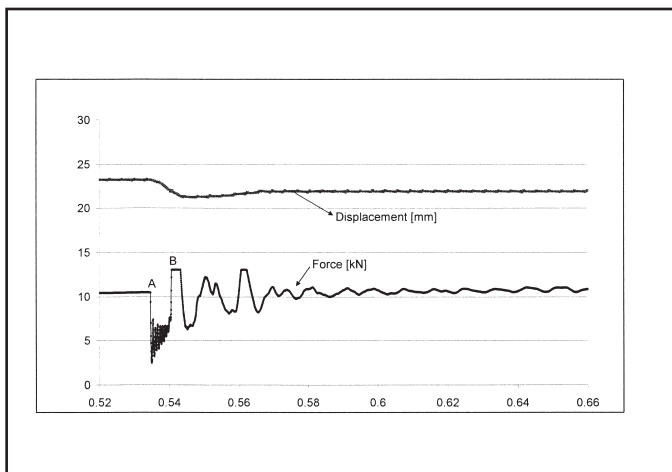


Fig. 9 — Data sample in supported breaking test.

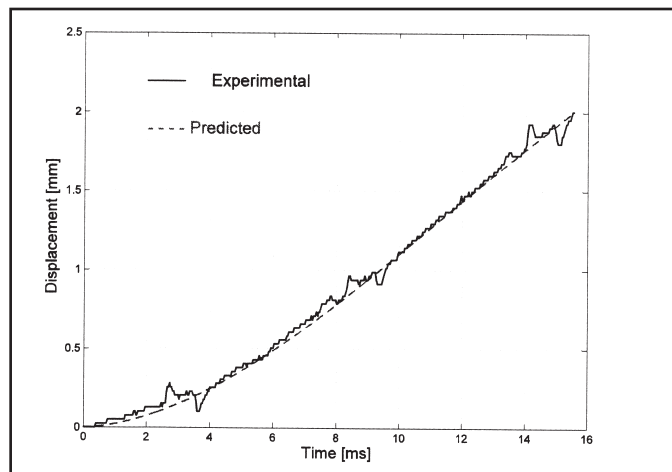


Fig. 10 — Example of experimental and predicted displacement at a load of 6.52 kN.

kN/mm. These tests, named “supported breaking tests,” correspond to normal welding operations, where a remaining reaction force exists during collapse of the projection. The springs are slightly pre-loaded ensuring a small reaction force on the moving electrode just after pin fracture. All in all 12 supported breaking tests were carried out in the load range 4.5–10.9 kN. It should be noted that the load F in Equation 1 in these experiments is the total action force just before pin fracture. Due to the slight loading of the springs before breaking of the pin, this total load is greater than net pin breaking force.

Figure 9 shows an example of the load and displacement curves, where fracture occurs at a total load of 10.5 kN. After fracture the force drops abruptly and then increases linearly with superimposed fluctuations due to the springs (curve part AB). The relative displacement of the electrodes is determined theoretically by inserting the values of m , b , and k identified by the free

breaking tests and the measured, oscillating force F into Equation 1. Solving for x is a vibration problem of one degree of freedom under the excitation of an arbitrary force. The solution is the well-known Duhamel’s integral (Ref. 12). The solution was obtained by numerical integration based on trapezoidal approximation.

A series of tests carried out with different fracture loads and reaction forces (different setup of springs) shows good agreement between experimental and predicted displacement curves. Figure 10 gives an example of comparison at a load $F = 6.52$ kN.

Projection Welding Tests

To further verify the model, a series of projection welding tests was carried out using the same AC machine as earlier, joining rings in stainless steel sheet (W.Nr. 1.4301) with disks in mild steel (W.Nr. 1.0037) provided with an annular projection — Fig. 11. An electrode force of 4.4 kN was

chosen, the weld time was 4 cycles, and the current was selected just below or just above the expulsion limit causing splash formation. During the experiments, the electrode force, the relative displacement between the two electrodes, and the weld current were recorded. An example of the data recorded is shown in Fig. 12. The weld stage part ranging from time A to B in Fig. 12 was selected for subsequent analysis.

Reading from Fig. 12, the electrode force prior to current flow $F = 4.5$ kN, and the measured reaction force F_r as function of time during the weld stage and inserting into the mathematical model Equation 1, the relative displacement was computed.

Figure 13 gives two examples on comparison between predicted and measured relative electrode displacement during the weld stage showing reasonable agreement.

Conclusions

The structure of the mechanical system